Cytometry
PART A
Journal of the International Society for Advancement of Cytometry

Imaging Mass Cytometry

Qing Chang,[1] Olga I. Ornatsky,[1] Iram Siddiqui,[2] Alexander Loboda,[1] Vladimir I. Baranov,[1] David W. Hedley[3]*

[1]Fluidigm Canada Inc., Markham, Ontario, L3R 4G5, Canada

[2]Department of Pathology, Hospital for Sick Children, Toronto, Ontario, M5G 1X8, Canada

[3]Division of Medical Oncology and Hematology, Princess Margaret Cancer Centre, Toronto, Ontario, M5G 2M9, Canada

Received 13 October 2016; Revised 13 December 2016; Accepted 28 December 2016

*Correspondence to: David Hedley, Division of Medical Oncology and Hematology, Princess Margaret Cancer Centre, 610 University Avenue, Toronto, Ontario M5G 2M9, Canada.
E-mail: david.hedley@uhn.ca

Conflict of Interests: O.O and V.B. are co-founders of DVS Sciences Inc. (now part of Fluidigm) which invented, developed and manufactures mass cytometry technologies including the Helios™ CyTOF System, the Imaging Mass Cytometer and metal-conjugated reagents.

Published online 3 February 2017 in Wiley Online Library (wileyonlinelibrary.com)

DOI: 10.1002/cyto.a.23053

• **Abstract**

Imaging Mass Cytometry (IMC) is an expansion of mass cytometry, but rather than analyzing single cells in suspension, it uses laser ablation to generate plumes of particles that are carried to the mass cytometer by a stream of inert gas. Images reconstructed from tissue sections scanned by IMC have a resolution comparable to light microscopy, with the high content of mass cytometry enabled through the use of isotopically labeled probes and ICP-MS detection. Importantly, IMC can be performed on paraffin-embedded tissue sections, so can be applied to the retrospective analysis of patient cohorts whose outcome is known, and eventually to personalized medicine. Since the original description in 2014, IMC has evolved rapidly into a commercial instrument of unprecedented power for the analysis of histological sections. In this Review, we discuss the underlying principles of this new technology, and outline emerging applications of IMC in the analysis of normal and pathological tissues. © 2017 International Society for Advancement of Cytometry

• **Key terms**

mass cytometry; image analysis; systems biology; hypoxia; cell signaling

Underlying Principles of Imaging Mass Cytometry

In mass cytometry, single cells labeled with antibodies or other probes carrying a high mass tag undergo ionization in an inductively coupled plasma, with the ions from each cell measured by time of flight (TOF) mass spectrometry (1–5). High-content analysis is enabled by conjugating antibodies to metal-chelating polymers carrying stable isotopes from the lanthanide series, with the data collected displayed and analyzed similar to high-parameter flow cytometry. Imaging mass cytometry (IMC), which was described originally in a recent publication (6), introduced the adaptation of a novel laser ablation device to the mass cytometer. Tissue sections or cells immobilized on slides are stained with panels of antibodies and other probes, and inserted into an ablation chamber where the tissue is scanned by a pulsed laser operating at 213 nm and focused to a 1 μm diameter spot size. Tissue from an ablation spot is vaporized on each laser shot, and is carried by a stream of inert gas with high time-fidelity into the inductively coupled plasma ion source for simultaneous analysis by the mass cytometer (Fig. 1). The metal isotopes associated with each spot are simultaneously measured and indexed against the location of each spot. The tissue is scanned spot-by-spot along a scan line while the slide is moved under the fixed laser beam; sequential scan lines ultimately yield an intensity map of all target proteins throughout the tissue or the region of interest.

It follows that the use of a smaller laser spot size improves spatial resolution at the expense of reduced sensitivity, as fewer ions are collected from each spot, and reduced image acquisition time. Higher speed (or increased laser ablation spots per second) increases the speed of image acquisition, but also increases the probability of material cross contamination between spots. The images used to illustrate this Review were acquired using a 1 μm spot size. The rastering speed of 200 pixels/s (or

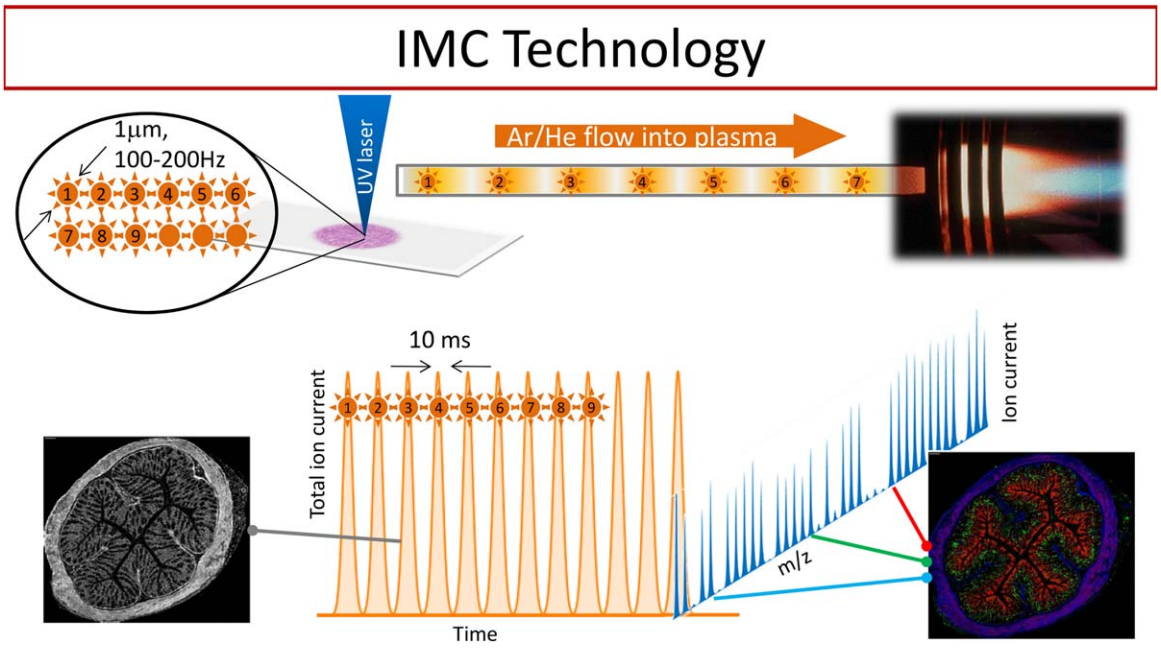

Figure 1. Schematic of IMC. Ablation of tissue sections is achieved using an autostage and a pulsed 213 nm laser, focused to a 1 μm spot size and operating at 100–200 Hz. Each laser shot produces a plume of particles that are carried to the mass cytometer by a stream of inert gas. Raster scanning produces an image where the ion current for each mass tag gives an indication of its abundance, whereas the gray-scale image provided by the total ion current provides anatomical detail. [Color figure can be viewed at wileyonlinelibrary.com]

laser ablation spots per second) resulted in <2% cross contamination between spots, which produced sharp-contrast images. At this speed and laser spot size, one square millimeter sample area can be scanned in <2 h. The addressable sample size on a slide is 5 mm × 30 mm, which can be optically examined with an integrated 20× objective to define regions of interest for ablation.

Multiplexed ion beam imaging (MIBI) is an alternative approach to imaging histological sections labeled with mass-tagged antibodies, under development by Nolan and co-workers (7). In contrast to the IMC, which is essentially an atmospheric laser ablation chamber interfaced to a mass cytometer, MIBI uses an oxygen primary ion beam to rasterize sections under vacuum, releasing showers of secondary ions from the antibodies. These are analyzed by a mass spectrometer equipped with multiple detectors, allowing the detection of up to 7 antibodies per sweep of the ion beam. A recent review by Bodenmiller compares the imaging characteristics of IMC and MIBI to those of immunofluorescence, in terms of sensitivity, resolution, complexity, and throughput (8). Although the physical principles of extracting material from tissue sections by IMC and MIBI are different, both methods use antibodies conjugated to stable metal isotopes developed for mass cytometry, are quantitative and their application, which is the main focus of this Review, is similar. Importantly, similar to immunohistochemistry, IMC and MIBI can be applied to formalin-fixed, paraffin-embedded (FFPE) tissue sections. As well as lending itself to standard pathology samples, the use of archival paraffin blocks allows the retrospective study of patient cohorts. This will greatly enhance their clinical utility, since it will allow the identification of molecular signatures, defined in high-parameter space, predictive of response to targeted agents, and patient outcome.

Yet another mass spectrometry based technique, Matrix-Assisted Laser Desorption/Ionization (MALDI) tissue imaging, should be mentioned. It is a well-established technique especially beneficial when previous knowledge about the sample is absent (9). De novo investigation of the molecular content of tissues preserving its morphological context is a very attractive goal, and the method employs a broad spectrum of mass analyzers including the most conventional TOF (10), and less common Fourier Transform-Ion Cyclotron Resonance (11) and Orbitrap (12). MALDI resolution is approaching 3–5 μm. Recently, the analysis of FFPE tissue samples attracted significant attention due to availability and fundamental importance of samples (12,13).

Stains and Probes

Mass cytometry is based on the use of antibodies conjugated to polymers incorporating a chelating agent specific to a given element, and capable of carrying an average of ~160 atoms/antibody molecule (14). They are labeled using stable isotopes primarily from the lanthanide series. There are 37 of these commercially available, with additional non-lanthanide metal tags (bismuth, gold, platinum), which sets an upper limit of 40 antibodies that currently can be combined in a staining protocol. Further advances in polymer chemistry will likely extend this considerably through the incorporation of additional elements. Many of the antibody conjugates against

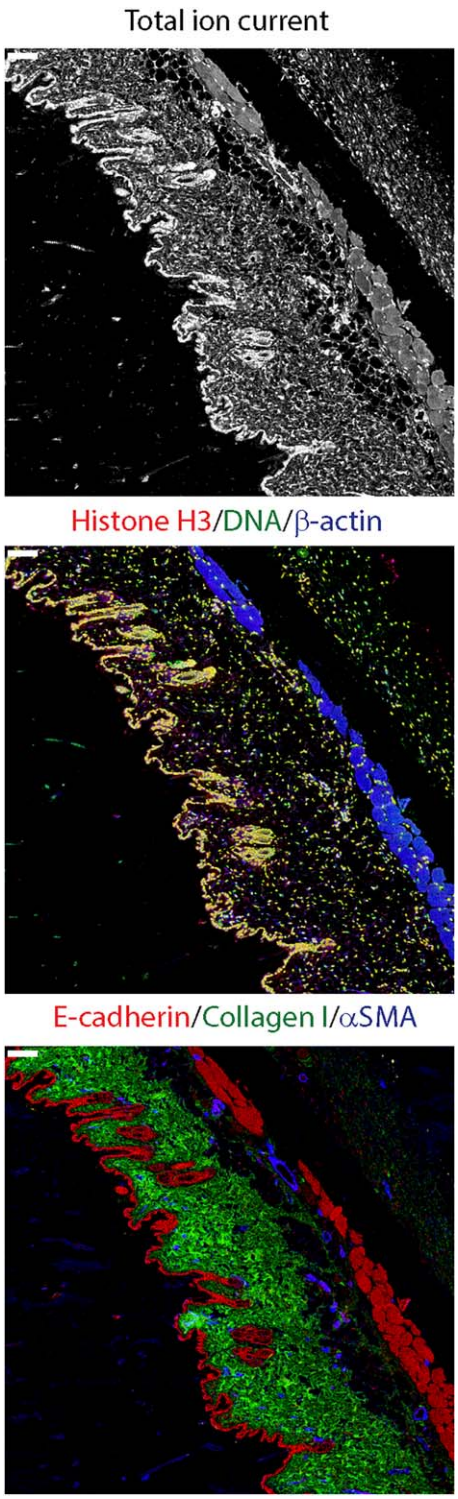

Figure 2. Full-thickness IMC image of normal mouse abdominal wall, showing the different anatomical layers. Top panel, total ion current; Middle panel, β-actin, histone H3 and Iridium intercalator; Bottom panel, E-cadherin, collagen and αSMA. Note that the epidermis stains strongly for E-cadherin and the nuclear markers histone H3 and DNA (shaded yellow); the dermis for collagen I; blood vessels running through the subcutaneous fat are αSMA-positive, and the abdominal wall striated muscle for E-cadherin and β-actin. [Color figure can be viewed at wileyonlinelibrary.com]

intracellular markers prepared for mass cytometry, which analyzes cells in suspension, can be used for IMC. However, this is not always the case, and a general rule of thumb appears to be that antibodies that work well with immunohistochemistry are likely to be successful with IMC. In addition to metal-tagged antibodies, there is clear potential to develop oligonucleotide probes for IMC for gene transcription analysis.

"Navigational aids"

Tissue sections, particularly those obtained from cancer, are complex structures. In addition to a heterogeneous mix of cellular elements, components such as extracellular matrix and blood vessels play key roles in tissue organization and function. We use the term navigational aids to describe features used for the initial orientation and segmentation of IMC images, prior to detailed cellular analysis. One of the most useful of these is the total ion current, which sums all ion signals arriving at the detector, and gives a grayscale image (Fig. 2). Iridium- and rhodium-containing DNA intercalators are extensively used in conventional mass cytometry for cell counting and live/dead discrimination (15). When applied to IMC they play additional roles, providing information about nuclear size, shape and texture that can be used to classify cells (analogous to chromogenic nuclear stains used in light microscopy), and for measuring the nuclear/cytoplasmic distribution of intracellular proteins. The use of metal-tagged anti-histone H3 for nuclei was described by Giesen et al. (6), and can be combined with Ir- or Rh-intercalators, as illustrated in Figure 2.

Functional Markers

These are tracers administered in vivo to track biochemical processes. The best-characterized is the thymidine analogue iododeoxyuridine (IdU) that is taken up, phosphorylated, and incorporated into DNA during S-phase. Recently Nitz and co-workers at the Department of Chemistry, University of Toronto, have been developing functional probes for mass cytometry based on the organic chemistry of tellurium (16). Using isotopically pure tellurium, they have been able to synthesize "isotopologues," probes that have identical structure and pharmacology but are readily separated by mass of the tellurium isotopes. This opens the possibility for unique biochemical studies at the intact tissue level using pulse/chase techniques, as shown in a recent article by this group describing temporal fluctuations in tumor hypoxia using 2-nitroimidazole tracers incorporating different tellurium isotopes (17). Our group has also used IMC to measure the biodistribution of the chemotherapy agent cisplatin in patient-derived xenografts (18), and more recently in specimens from patients who received cisplatin (unpublished). In both instances a striking and unanticipated finding was the extensive binding of Pt to collagen fibers in the tumor, as well as in normal tissues; an observation that is highly relevant to our understanding of the pharmacology of this important anti-cancer agent.

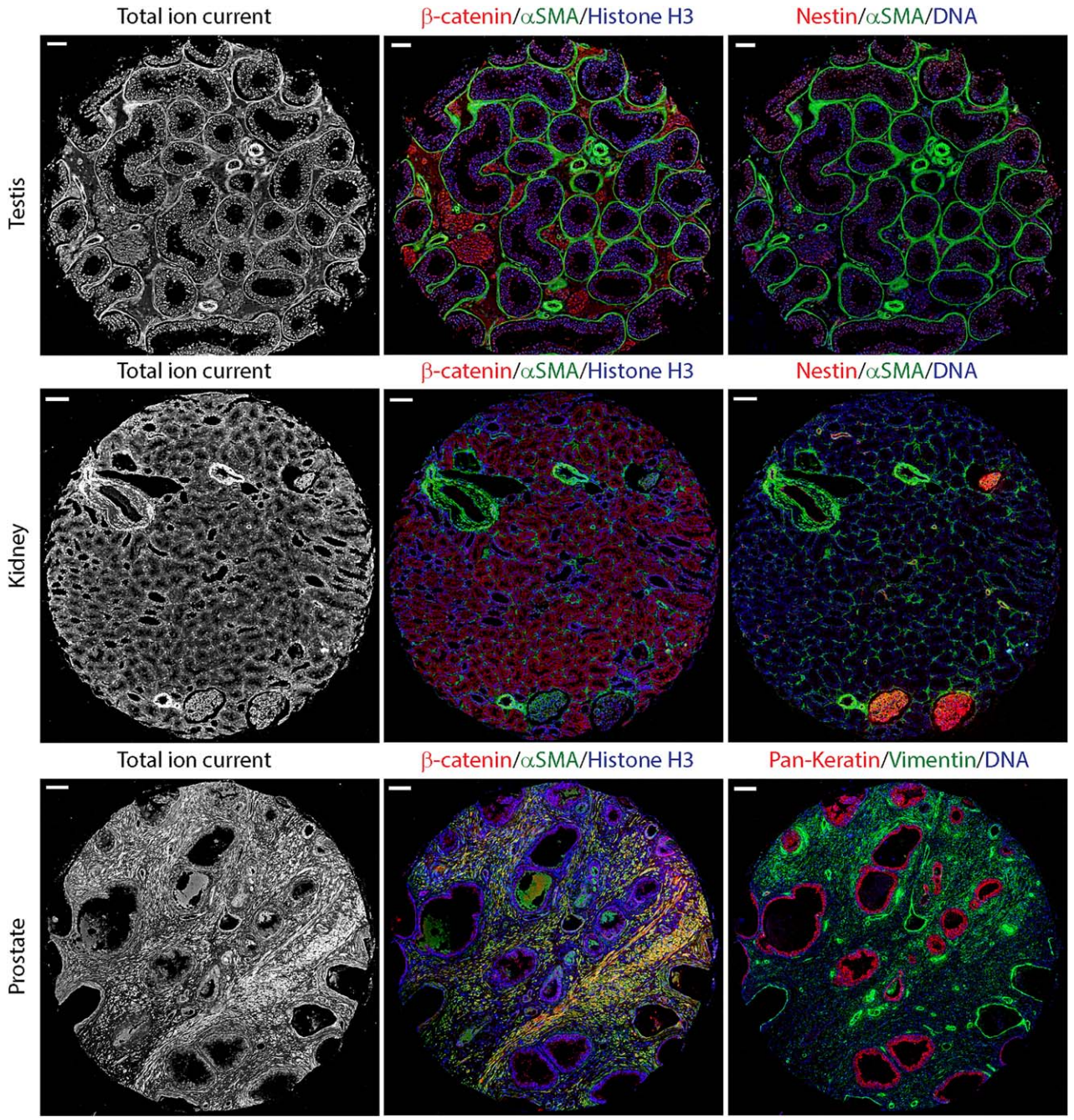

Figure 3. IMC patterns for normal human testis, kidney, and prostate, obtained from a tissue microarray. The total ion current for each organ is shown in the left columns, and the RGB images are based on combinations of individual antibodies imaged by IMC, chosen to highlight normal anatomical features of each organ. [Color figure can be viewed at wileyonlinelibrary.com]

Data Analysis and Quantitation

The high-dimensional data sets generated by IMC and MIBI require software tools that provide interpretation and visualization of tissue samples with localization of all markers, quantitative measurements at the tissue, cellular, and subcellular levels. Both techniques give a linear signal over a much higher dynamic range than immunohistochemistry or immunofluorescence, and because the number of ions arriving at the detector can be normalized by reference to standards with known concentration of labeling isotopes, they can measure the relative amounts of bound antibody.

Powerful, sophisticated algorithms are necessary to visualize the extensive per-cell multidimensional data in a tissue section. Computer-generated images co-register all of the markers in high-dimensional space and are amenable to analysis using third-party software. Currently we use the Definiens® Developer XD platform for digital pathology (Definiens AG; Munich, Germany), which has machine

learning capability for the automatic segmentation and classification of individual cells, using rule sets developed in close collaboration between a pathologist and programmer (18). Since the first step in the analysis is segmentation of the image into single cells, antibody panels include cell membrane, nuclear and stromal markers. Using the Developer XD, data for each cell can be mapped directly onto the tissue sections to determine marker intensity, intensity statistics within compartments, morphology parameters such as size and shape, spatial correlates, and contextual parameters such as epithelium versus stroma (18). Alternative approaches to the analysis of high content IMC and MIBI images are described by the Nolan and Bodemiller groups (7,19).

In contrast to flow cytometry, where isolated whole cells are analyzed, in tissue sections, cells often overlap and are packed together, and may be cut through at an angle whereby they are seen only as fragments. Thus, clusters in scatter plots for data from tissue sections are not nearly as well-defined as they are in flow cytometry analysis. As a result, cell classifications in tissue sections cannot be as precise as in flow cytometry. This problem can be addressed by including multiple markers against the cell population of interest.

Application of IMC

The images used to illustrate this review article, are the result of collaboration between the Hedley group at the Princess Margaret Cancer Centre, Toronto, ON, Canada and the team at Fluidigm Canada Inc., Markham, ON, Canada, and were acquired using prototypes of a commercial imaging mass cytometer. Their purpose is to point the reader toward the huge untapped potential of this technology, and to supplement the recent publications from the Bodenmiller group at the University of Zurich, who pioneered application of IMC (6,8,19). It should be appreciated that these illustrations are taken from files based on 20–30 individual markers, and that the RGB rendering is based on the selection of three markers at a time for pseudo-color visualization and does not reflect the true complexity of the data.

Application to Normal Tissues

Although the main application of IMC is likely to be the study of diseased tissues, especially cancer, it can also provide a unique window into the structure and function of normal tissues, which is easier to appreciate than the highly deranged features that are typical of cancer.

Normal mouse skin. Figure 2 illustrates normal mouse skin, taken from the abdomen and including all layers down to the abdominal wall striated muscle. The top panel is the total ion current. The middle panel shows dual representation of the iridium intercalator and anti-histone H3, and illustrates that, as expected, the two nuclear markers co-localize as indicated by the yellow color. The underlying abdominal wall muscle is clearly labeled with anti-β-actin. In the bottom panel the epidermis and hair follicles are strongly stained for E-cadherin, as is the muscle layer, and the dermal collagen is clearly seen. Blood vessels running in the subcutaneous fat are labeled with anti-α-smooth muscle actin (αSMA).

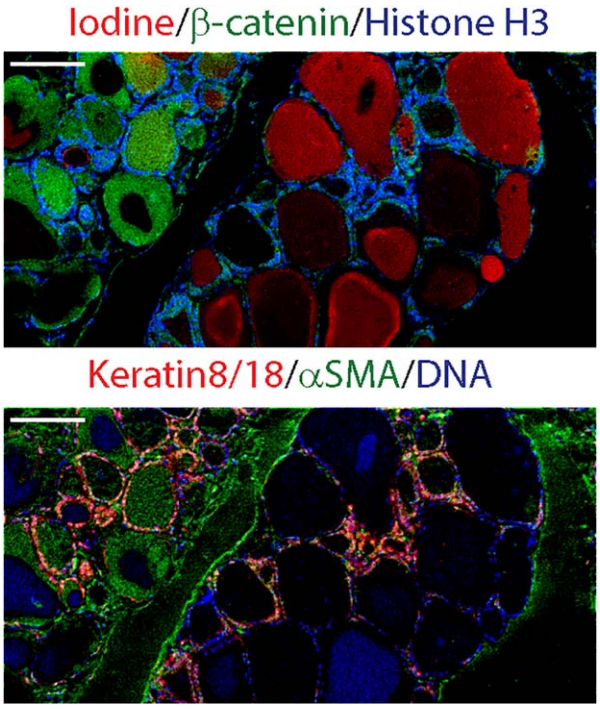

Figure 4. IMC images of normal human thyroid gland, showing direct imaging of the ^{127}I-iodine containing thyroid hormone (top panel). [Color figure can be viewed at wileyonlinelibrary.com]

Normal human testis, kidney, and prostate. Figure 3 is based on a normal human tissue microarray, stained with a panel of markers designed to illustrate the similarities and differences in these three tubular structures. In the testis, the basement membrane is clearly outlined by αSMA, with surrounding β-catenin-positive interstitial cells. In the kidney, the arterioles are outlined by αSMA, and glomeruli label strongly for the intermediate filament nestin, which plays a key role maintaining the cytoskeleton of podocytes (20). In the prostate, αSMA and β-catenin appear co-localized in the stroma, and the glandular epithelium stains strongly for pan-keratin, surrounded by vimentin-positive mesenchymal cells.

Normal human thyroid gland. The bulk of the thyroid gland consists of follicles lined by a cuboidal epithelium that traps iodine, and incorporates it into thyroid hormones, which are stored bound to thyroglobulin in the colloid that fills the follicles. In Figure 4, we used the unique ability of IMC to directly image the iodine-I^{127} atoms in normal thyroid. In this example, there appears to be considerable variability in the amount of iodine in the individual thyroid follicles.

Normal mouse intestine. Here we introduce the use of IdU incorporation as a functional probe for DNA synthesis. In Figure 5, the epithelial lining of both the small intestine and the

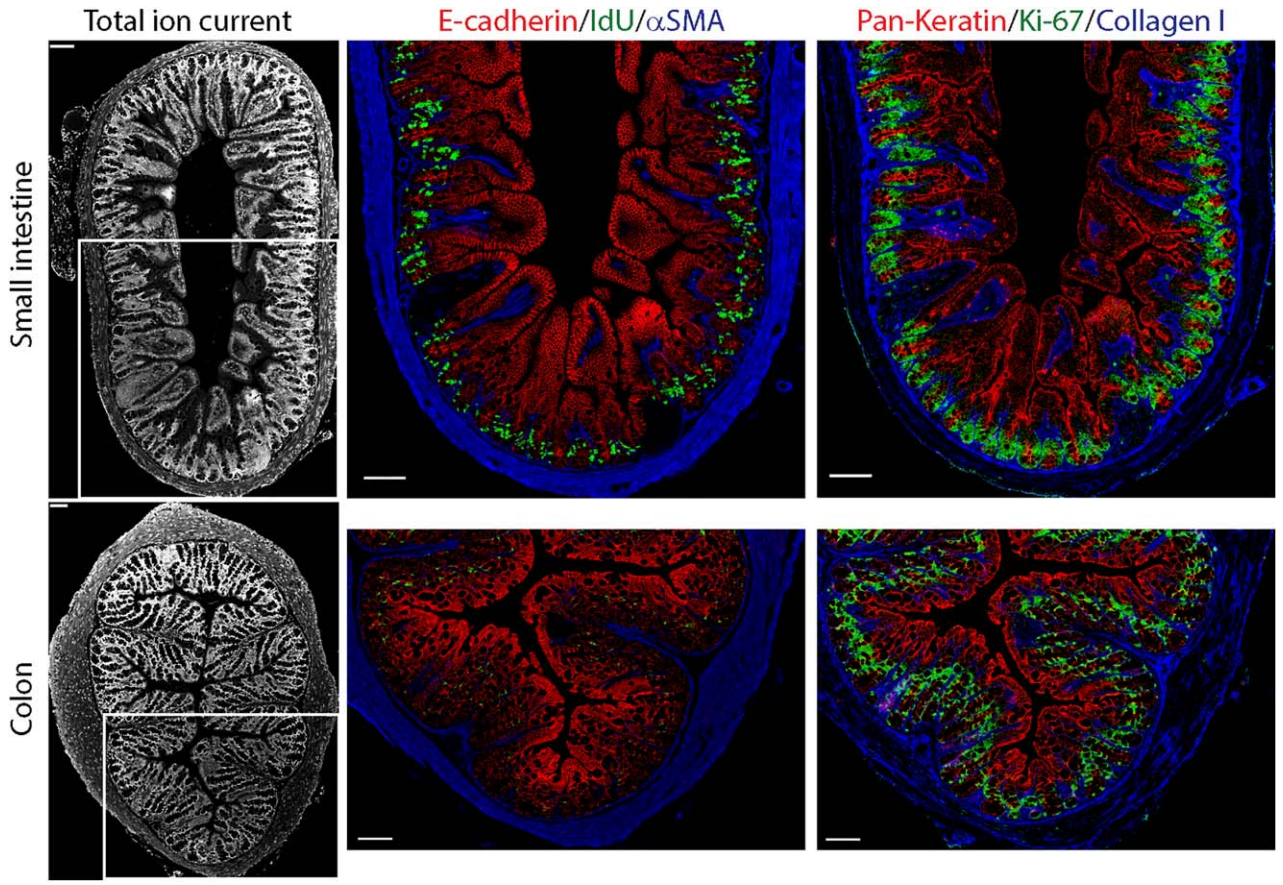

Figure 5. IMC images of normal mouse small intestine (top panels) and colon (bottom panels). The mice were given a single injection of IdU 30 min before sacrifice, and its incorporation into DNA is readily seen in the basal crypt cells of the small intestine, and to a lesser extent in the colon. The proliferation marker Ki-67 (right panels) shows a similar distribution pattern to IdU, but staining is much more extensive, consistent with its lack of cell cycle phase specificity. [Color figure can be viewed at wileyonlinelibrary.com]

colon is seen to stain prominently with antibodies to E-cadherin on the outer membrane and intracellular cytokeratin, whereas the intestinal wall and central core of the villous lamina propria are labeled with anti-αSMA and collagen I. IdU 60 mg/kg was administered by intraperitoneal injection 30 min prior to sacrifice, and is seen to be taken up by small intestinal basal crypt epithelial cells, but not by the surface epithelial cells in the villi (18). It also labels epithelial cells in the colonic mucosa, although to a lesser extent than that seen in the small intestine. For comparison, the sections were also stained for Ki-67, a proliferation marker used extensively in surgical pathology. It can be seen that the distribution pattern of Ki-67 is similar to that of IdU. However, a greater proportion of epithelial cells is labeled in both the small intestine and the colon, consistent with the expression of Ki-67 in actively proliferating basal crypt epithelial cells, regardless of their cell cycle phase distribution, whereas IdU incorporation is confined to cells in S-phase.

Application to Cancer

Although we are now well into the era of genomics-based personalized cancer medicine, the percentage of patients whose outcome is meaningfully improved by treatments based on genomics data remains small. In part this is explained by the lack of effective drugs to target many of the important drivers of cancer growth, such as the loss of tumor suppressors and activating RAS mutations. Another major factor that is inadequately addressed by current genomics methods is the presence of tumor heterogeneity (21). Heterogeneity within individual tumors exists at the cancer cell level, and in the tumor microenvironment which broadly comprises stromal elements, blood vessels, and immune infiltrates. It seems intuitively obvious that the introduction of IMC into the pathology laboratory has enormous potential to transform clinical practice by addressing tumoral heterogeneity, providing as it does a platform that appears to align well both to cancer genomics, and to current histopathology practice (6,8). Furthermore, the highly multiplexed images created by IMC open the potential for a systems biology approach to cancer treatment, in which the individual elements of a regulatory pathway are captured, the nodal points of functional derangement pinpointed, and the appropriate treatment given (8).

At the time of writing very little work has been published describing the application of IMC to cancer. Our own group has a particular interest in pancreatic cancer, with a focus on the biology of tumor hypoxia, and on the preclinical

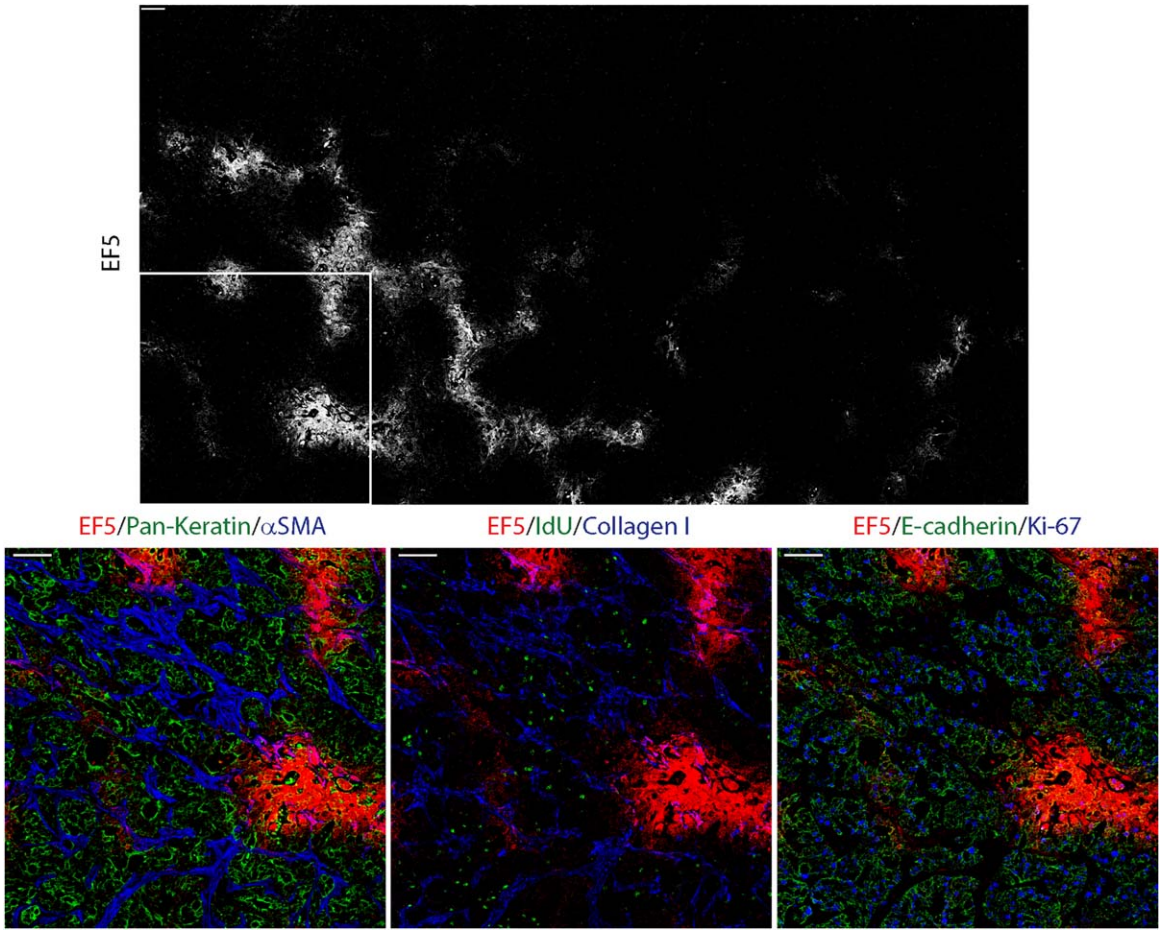

Figure 6. Distribution of hypoxia in a pancreatic cancer patient-derived xenograft, revealed using the 2-nitroimidazole tracer EF5. Top panel is the whole IMC image, showing a typical distribution of hypoxia, and the lower images are close-ups to illustrate some of the features of the hypoxic microenvironment. [Color figure can be viewed at wileyonlinelibrary.com]

development of molecular-targeted agents. Some of our recent unpublished work is used to illustrate the scope of IMC to study solid tumors.

Tumor hypoxia. Hypoxia probably develops to some degree in all solid tumors as the utilization of oxygen exceeds its supply by the inefficient tumor vasculature (22,23). High levels of hypoxia have long been associated with resistance to radiotherapy and chemotherapy, and more recently with greater metastatic potential (24). Hence there is interest in understanding the underlying mechanisms, and in the development of agents that selectively target hypoxic cells. Using xenografts derived from pancreatic cancer patients, we observed a striking correlation between hypoxia, rapid growth, and spontaneous metastasis (25). We are in the process of completing a clinical study that involves the administration of the hypoxia tracer pimonidazole to a cohort of 100 patients undergoing pancreatectomy, to establish if hypoxia predicts poor outcome in patients (26). To elucidate the underlying mechanisms, we are developing IMC protocols incorporating mass-tagged anti-pimonidazole into panels of antibodies to study regulatory pathways that promote hypoxia tolerance and/or aggressive growth. These include alterations in metabolism, signaling pathways, cell cycle control, and antioxidant systems. Figure 6 shows some of our early data, with a map showing the distribution of hypoxia in the entire IMC image, zooming in on a region that contains both hypoxic and well-oxygenated viable tumor tissue. In this figure, we show the distribution of hypoxia in relation to cancer cells (pan-keratin- and E-cadherin-positive) and mesenchymal cells (αSMA-positive), to IdU uptake, and to Ki-67. Note that both of these markers of proliferation show low expression in regions of hypoxia.

Cell signaling pathways. Aberrant activation of signaling pathways, for example due to overexpression of surface growth factor receptors or mutations in pathway elements, plays a major role in cancer development and progression. Abnormal signaling can be readily detected in patient samples by staining with the appropriate phosphospecific antibodies. However, despite an intense effort treating cancer patients with pharmacological inhibitors of these pathways, relatively little headway has been made improving long- term survival. To a large extent treatment failure is likely explained by redundancies and feedback loops in signaling pathways. High-

content analysis by mass cytometry, incorporating large numbers of phosphospecific antibodies, gives a more complete assessment of the organization of signaling networks (2,4,27), but the requirement for fresh patient samples makes it difficult to accrue sufficient patients with follow-up to assess the clinical relevance. Given the comprehensive range of phosphospecific antibodies suitable for immunohistochemistry, it is likely that IMC will emerge as a powerful technique for understanding how derangements in cell signaling promote cancer progression, and for the identification of vulnerabilities that can be selectively targeted by drugs. Figure 7 illustrates IMC analysis of samples from an experiment testing combined inhibition of the ERK and mTOR pathways in pancreatic cancer xenografts (28), using a panel of mass-tagged phosphospecific antibodies and the proliferation marker Ki-67. In the control tumors, both ERK and the mTOR target S6 ribosomal protein are strongly phosphorylated and Ki-67 labeling is high, consistent with the aggressive biology of these cancers. In this example, combined treatment with MEK and mTOR inhibitors almost completely suppresses ERK and S6 phosphorylation, and results in a large decrease in Ki-67 labeling.

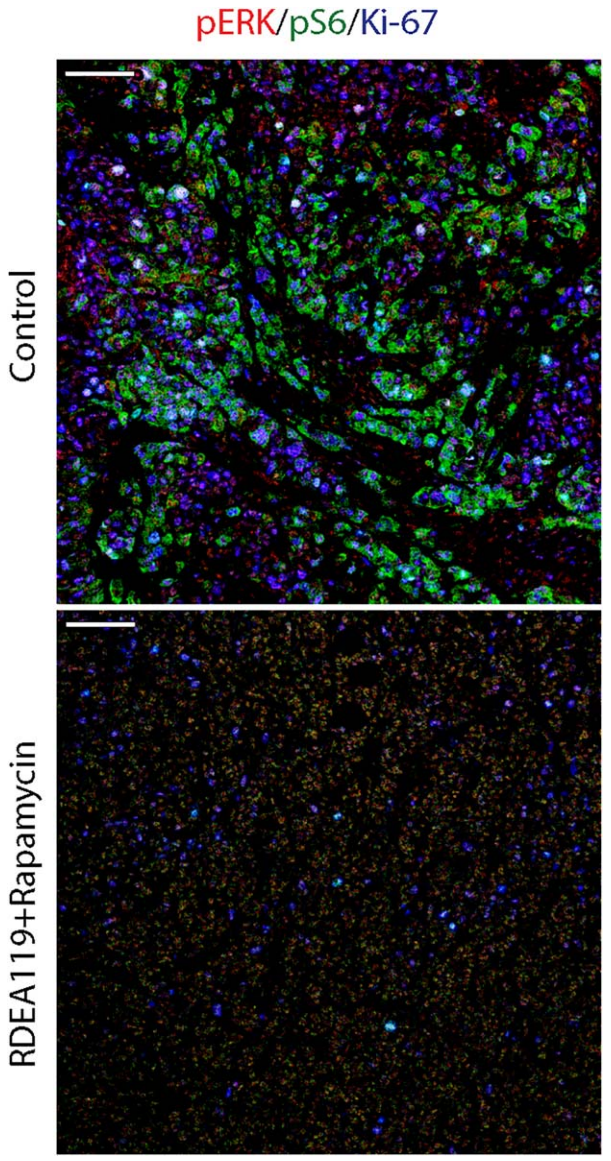

Figure 7. Combined labeling for phosphorylated ERK and S6 ribosomal protein, and the proliferation marker Ki-67 in a pancreatic cancer patient-derived xenograft (top panel). The lower panel is from a second tumor where the host mouse was treated with the MEK inhibitor RDEA119 to inhibit the ERK pathway and the mTOR inhibitor rapamycin. Dual treatment with these signal transduction inhibitors profoundly suppresses the pathways, and is associated with cell cycle arrest. [Color figure can be viewed at wileyonlinelibrary.com]

Opportunities and Challenges Moving Forward

Opportunities

Even at this early phase of developing IMC and MIBI applications, these are clearly very powerful analytical platforms that successfully couple high-density analysis by mass cytometry to conventional histology, with truly transformational potential in cancer pathology (7,8). This potential is enhanced by the ability to image standard paraffin sections at near-optical resolution, as IMC can be applied to samples from groups of patients matched for tumor type, stage and treatment, whose clinical outcome is known. Furthermore, it is likely that the information obtained from IMC analysis of a cancer will be highly complementary to that from genomics techniques that are beginning to transition from research to routine clinical application. Increasingly the role of cancer pathology is shifting from refinement of a diagnostic category toward individualized treatment selection. Given the high cost of some of the newer anticancer agents, the successful implementation of IMC in a clinical facility would likely make economic sense, on top of the potential benefit to patient care and basic science. Another major area for development that is not touched on in this review is the burgeoning field of immune-oncology, where the ability to classify infiltrating immune cells in high-parameter space while maintaining their spatial coordinates is likely to yield new insights into host responses, and potentially guide the selection of appropriate immunotherapy treatment.

Although we have focused on the application of IMC to cancer, the examples of normal tissue analysis by IMC used to illustrate this review point toward a much wider potential, for example in the elucidation of the underlying mechanisms in areas such as non-malignant pathology and normal tissue physiology. As a research tool IMC could in principle be applied across the entire spectrum of multicellular organisms, including plants, and it seems likely that these fields will be explored as the technology matures.

Challenges

The sheer scope of high-content analysis of intact tissues at the single-cell level appears to be the greatest single challenge to the effective implementation of IMC, and efficient experimental design will be critical in order to meet this. In particular, its potential for open-ended discovery research is virtually limitless, so that sorting results that are biologically

relevant from the huge number of "lstatistically significant" findings generated by a 40-antibody IMC experiment will need experience and critical thinking. As pointed out by Giessen et al. (6), IMC lends itself to a systems biology approach to histological sections due to its unique ability to cluster markers that define regulatory pathways, and that would seem a productive direction, providing as it does a natural link to hypothesis-driven research.

At the present time most of the metal-tagged antibodies available for mass cytometry are optimized for single-cell suspension analysis, and might be unsuitable for the corresponding epitope in tissue sections. In any case, there is a clear need for a comprehensive range of antibodies for use in IMC, and a considerable effort required to develop, optimize, and verify these. Catena et al. have developed a cloud-based platform, AirLab, for organizing these data and maintaining inventory in-house, which allows data sharing between individual laboratories and institutions (29). During the early dissemination of IMC technology such a platform would be invaluable. Although at the present time most of the effort has been directed toward antibodies, it is likely that reagents and protocols for nucleic acid detection by IMC will be developed over the next few years.

A fundamental limitation of IMC and MIBI is that, relative to optical techniques, the rate of image acquisition by laser ablation is slow (1.5 mm^2 in 2 h), and sets a practical limit to the extent to which a slide can be scanned. Many tissue markers of clinical importance show considerable intratumoral heterogeneity in their distribution patterns, so that failure to account for this results in sampling error (30). To a large extent this can be addressed by staining a section from the same block using immunohistochemistry directed to the marker of interest, and using that as a template to select representative regions of interest for laser ablation. This is facilitated by an optical imaging module incorporated into the ablation chamber. Furthermore, the ability to automatically ablate many chosen regions of interest within the full ablation area provides a solution. Although MIBI is still in development, it appears capable of faster image acquisition than IMC for the same number of markers (7 antibodies simultaneously), but as more markers are added, longer acquisition times are required for MIBI acquisition. It will be interesting to see how this technology develops over the next few years into a commercial product for the broader research community.

The analysis of highly multiplexed images acquired using IMC remains a challenge, but it appears to fall naturally into a number of steps. The first of these involves visual inspection, ideally by a group of experts that includes a pathologist. There is a practical limit to the number of markers that can be combined for visual inspection on a computer screen, but through the use of visualization tools all of the individual images in the file can be addressed in combinations determined by the user, to allow a verbal description of the features of interest. Computerized image analysis involves the automated classification and segmentation of intact cells, nuclei, or other objects of interest, followed by quantification of the expression level of each of the 40 markers. The high-dimensional single-cell/object data thus generated can then be addressed using tools similar to those used for high parameter flow/mass cytometry data (4). Clusters of interest can then be projected back onto the original image to allow their anatomical relationships to be identified. The ability of IMC data analysis to go back and forth between digital pathology and high-dimensional single-cell analysis appears to have enormous underexplored potential.

Literature Cited

1. Bandura DR, Baranov VI, Ornatsky OI, Antonov A, Kinach R, Lou X, Pavlov S, Vorobiev S, Dick JE, Tanner SD. Mass cytometry: Technique for real time single cell multitarget immunoassay based on inductively coupled plasma time-of-flight mass spectrometry. Anal Chem 2009;81:6813–6822.
2. Bendall SC, Simonds EF, Qiu P, Amir e, Krutzik PO, Finck R, Bruggner RV, Melamed R, Trejo A, Ornatsky OI, et al. Single-cell mass cytometry of differential immune and drug responses across a human hematopoietic continuum. Science 2011;332:687–696.
3. Ornatsky O, Bandura D, Baranov V, Nitz M, Winnik MA, Tanner S. Highly multiparametric analysis by mass cytometry. J Immunol Methods 2010;361:1–20.
4. Spitzer MH, Nolan GP. Mass cytometry: Single cells, many features. Cell 2016;165: 780–791.
5. Tanner SD, Baranov VI, Ornatsky OI, Bandura DR, George TC. An introduction to mass cytometry: Fundamentals and applications. Cancer Immunol Immunother 2013;62:955–965.
6. Giesen C, Wang HA, Schapiro D, Zivanovic N, Jacobs A, Hattendorf B, Schuffler PJ, Grolimund D, Buhmann JM, Brandt S, et al. Highly multiplexed imaging of tumor tissues with subcellular resolution by mass cytometry. Nat Methods 2014;11:417–422.
7. Angelo M, Bendall SC, Finck R, Hale MB, Hitzman C, Borowsky AD, Levenson RM, Lowe JB, Liu SD, Zhao S, et al. Multiplexed ion beam imaging of human breast tumors. Nat Med 2014;20:436–442.
8. Bodenmiller B. Multiplexed epitope-based tissue imaging for discovery and healthcare applications. Cell Syst 2016;2:225–238.
9. Crecelius AC, Schubert US, von EF. MALDI mass spectrometric imaging meets "omics": Recent advances in the fruitful marriage. Analyst 2015;140: 5806–5820.
10. Caprioli RM, Farmer TB, Gile J. Molecular imaging of biological samples: Localization of peptides and proteins using MALDI-TOF MS. Anal Chem 1997;69:4751–4760.
11. Becker JS, Zoriy MV, Pickhardt C, Palomero-Gallagher N, Zilles K. Imaging of copper, zinc, and other elements in thin section of human brain samples (hippocampus) by laser ablation inductively coupled plasma mass spectrometry. Anal Chem 2005; 77:3208–3216.
12. Ly A, Buck A, Balluff B, Sun N, Gorzolka K, Feuchtinger A, Janssen KP, Kuppen PJ, van de Velde CJ, Weirich G, et al. High-mass-resolution MALDI mass spectrometry imaging of metabolites from formalin-fixed paraffin-embedded tissue. Nat Protocol 2016;11:1428–1443.
13. Buck A, Balluff B, Voss A, Langer R, Zitzelsberger H, Aichler M, Walch A. How suitable is matrix-assisted laser desorption/ionization-time-of-flight for metabolite imaging from clinical formalin-fixed and paraffin-embedded tissue samples in comparison to matrix-assisted laser desorption/ionization-Fourier transform ion cyclotron resonance mass spectrometry?. Anal Chem 2016;88:5281–5289.
14. Majonis D, Herrera I, Ornatsky O, Schulze M, Lou X, Soleimani M, Nitz M, Winnik MA. Synthesis of a functional metal-chelating polymer and steps toward quantitative mass cytometry bioassays. Anal Chem 2010;82:8961–8969.
15. Ornatsky OI, Lou X, Nitz M, Schafer S, Sheldrick WS, Baranov VI, Bandura DR, Tanner SD. Study of cell antigens and intracellular DNA by identification of element-containing labels and metallointercalators using inductively coupled plasma mass spectrometry. Anal Chem 2008;80:2539–2547.
16. Edgar LJ, Vellanki RN, Halupa A, Hedley D, Wouters BG, Nitz M. Identification of hypoxic cells using an organotellurium tag compatible with mass cytometry. Angew Chem Int Ed Engl 2014;53:11473–11477.
17. Edgar LJ, Vellanki RN, McKee TD, Hedley D, Wouters BG, Nitz M. Isotopologous organotellurium probes reveal dynamic hypoxia in vivo with cellular resolution. Angew Chem Int Ed Engl 2016;55:13159–13163.
18. Chang Q, Ornatsky OI, Siddiqui I, Straus R, Baranov VI, Hedley DW. Biodistribution of cisplatin revealed by imaging mass cytometry identifies extensive collagen binding in tumor and normal tissues. Sci Rep 2016;6:36641.
19. Schuffler PJ, Schapiro D, Giesen C, Wang HA, Bodenmiller B, Buhmann JM. Automatic single cell segmentation on highly multiplexed tissue images. Cytometry Part A 2015;87A:936–942.
20. Wen D, You L, Zhang Q, Zhang L, Gu Y, Hao CM, Chen J. Upregulation of nestin protects podocytes from apoptosis induced by puromycin aminonucleoside. Am J Nephrol 2011;34:423–434.
21. Tannock IF, Hickman JA. Limits to personalized cancer medicine. N Engl J Med 2016;375:1289–1294.
22. Brown JM. Tumor microenvironment and the response to anticancer therapy. Cancer Biol Ther 2002;1:453–458.

23. Vaupel P, Mayer A. Tumor hypoxia: Causative mechanisms, microregional heterogeneities, and the role of tissue-based hypoxia markers. Adv Exp Med Biol 2016;923: 77–86.
24. Hill RP, Marie-Egyptienne DT, Hedley DW. Cancer stem cells, hypoxia and metastasis. Semin Radiat Oncol 2009;19:106–111.
25. Chang Q, Jurisica I, Do T, Hedley DW. Hypoxia predicts aggressive growth and spontaneous metastasis formation from orthotopically grown primary xenografts of human pancreatic cancer. Cancer Res 2011;71:3110–3120.
26. Dhani NC, Serra S, Pintilie M, Schwock J, Xu J, Gallinger S, Hill RP, Hedley DW. Analysis of the intra- and intertumoral heterogeneity of hypoxia in pancreatic cancer patients receiving the nitroimidazole tracer pimonidazole. Br J Cancer 2015;113: 864–871.
27. Bodenmiller B, Zunder ER, Finck R, Chen TJ, Savig ES, Bruggner RV, Simonds EF, Bendall SC, Sachs K, Krutzik PO, et al. Multiplexed mass cytometry profiling of cellular states perturbed by small-molecule regulators. Nat Biotechnol 2012;30:858–867.
28. Chang Q, Chapman MS, Miner JN, Hedley DW. Antitumour activity of a potent MEK inhibitor RDEA119/BAY 869766 combined with rapamycin in human orthotopic primary pancreatic cancer xenografts. BMC Cancer 2010;10:515.
29. Catena R, Ozcan A, Jacobs A, Chevrier S, Bodenmiller B. AirLab: A cloud-based platform to manage and share antibody-based single-cell research. Genome Biol 2016; 17:142.
30. Pintilie M, Iakovlev V, Fyles A, Hedley D, Milosevic M, Hill RP. Heterogeneity and power in clinical biomarker studies. J Clin Oncol 2009;27:1517–1521.